Singularities of Periodic Orbits near Invariant Curves

A. Celletti [a] and C. Falcolini [b]

[a] *Dipartimento di Matematica, II Università di Roma (Tor Vergata), Via della Ricerca Scientifica, 00133 Roma, Italy*

[b] *Dipartimento di Matematica, Università di Roma Tre, L.go S.L. Murialdo 1, 00146 Roma, Italy*

Abstract

We show numerically, for standard–like maps, how the singularities (in the complex parameter) of the function which conjugates the map to a rotation of rational period behave when the period goes to an irrational number. Furthermore, we propose a numerical method to extrapolate the radius of convergence of the series parametrizing the solution of periodic orbits. The results are compared with analyses performed by Padé approximants, Greene's method, root criterion and the prediction by renormalization theory.

1 Introduction

It is well known since Poincaré's conjecture that periodic orbits play an important role in the dynamics of conservative systems ([16]): " *... here is a fact that I have not been able to prove rigorously, but that seems to me very reasonable. Given Hamilton's equations and a particular solution of these equations, one can always find a periodic solution (whose period, it is true, can be very long) such that the difference between the two solutions may be as small as one wishes for as long as one wishes*". In particular, periodic orbits with large frequency may approximate the dynamics of an invariant curve with very high precision. This idea is at the basis of Greene's method ([10]), which aims to compute the break–down threshold of an invariant curve with irrational rotation number ω, using the stability properties of periodic orbits with frequency given by the rational approximants to ω. Such a method is very accurate and it has partially been proved theoretically ([8,15]). In particular, it is explained by a renormalization procedure based on rational approximation of irrational numbers ([14]). However, Greene's method does not provide informations about the location of the singularities of periodic orbits or the analyticity domain of invariant curves. More precisely, let us consider standard like mappings with perturbative parameter ε, where ε is assumed to be a complex number. Experimental evidence shows that Greene's value coincides with the distance to the origin of the closest singularity on the positive real axis of the complex ε–plane.

To get informations about the analyticity properties of periodic orbits or invariant curves one can compute Padé ([2]) approximants as in [4,5,9,12,7,6]. More precisely, we parametrize the solution of a periodic orbit with frequency $\frac{p}{q}$ (for some $p, q \in \mathbf{Z}_+$) by a $2\pi p$–periodic function $u(\varphi) = u(\varphi; \varepsilon)$ depending on a parametric coordinate φ whose flow is linear with frequency $2\pi\frac{p}{q}$. The function $u(\varphi)$ is analytic in ε and can be expanded in Taylor series as $u(\varphi;\varepsilon) \equiv \sum_{j=1}^{\infty} u_j(\varphi)\varepsilon^j$, where the coefficients $u_j(\varphi)$ can be recursively computed. If N terms of the previous sum (with N an even positive integer) are explicitely determined, Padé approximants can be computed up to the order $[N/2, N/2]$. This method has the big advantage to provide informations about the location of the corresponding $N/2$ singularities and thereby informations about the shape of the analyticity domain and its radius of convergence (as given by the closest singularity to the origin). However, we stress that Padé method presents serious limitations in concrete applications, due to the fact that to get reliable results one must use a precision of N decimal digits. In the present work we are forced to stop (by computer time limits) to the order [200/200]. The implementation of Padé method for invariant curves and their approximating periodic orbits provides informations about the way in which singularities of periodic orbits approach the analyticity domain of the invariant curve.

To overcome the limitations of Padé approximants, we present a new method which provides to high accuracy the analyticity radius within a short computer time. However, the information lost with respect to Padé method is the shape of the analyticity domain. The proposed method is based on the computation of a quantity, say $s_1 = s_1(\varepsilon)$, related to the numerical definition of Lyapunov exponents. From the graph of $s_1(\varepsilon)$ versus ε we can compute the analyticity threshold; an authomatic program has been developed to perform this task. Beside its fastness, the *Lyapunov* method has the further advantage to depend only on two parameters, namely the order N of the truncation of the power series expansion of the function $u(\varphi;\varepsilon)$ and the increment h in ε when computing the plot of s_1 versus ε. The dependence on both parameters is very straightforward. In particular, larger is N better is the accuracy of the computation. As for the increment h, we remark that it cannot be too large (to avoid loss of precision), nor too small (to reflect the accuracy of the computations). In all cases studied in this work, we have determined an almost optimal value as $h = 10^{-3}$.

We start our analysis by considering the Chirikov standard map and the golden mean case. Next we consider different irrational numbers and two more examples of standard–like maps. In all cases we find a good agreement between Padé and Lyapunov methods; they agree also with Greene's results whenever the analyticity domain is close to a circle (i.e., the intersection with the positive real axis almost coincides with the analyticity radius). A comparison with the (less precise) root criterion is also performed. As a byproduct of our computations, we determine by a linear fit the rescaling of the thresholds associated to the rational approximants to the irrational rotation number. For the golden mean rotation number all methods (Greene, Padé and Lyapunov) agree with renormalization theory predictions, since they rescale according to a factor coinciding with the largest eigenvalue of the unstable manifold of the critical fixed point. Two different rescalings are found as rotation numbers different from the golden ratio are investigated.

This paper is organized as follows: in §2 we provide the details to construct a perturbative series expansion for periodic orbits via a recursive algorithm. In §3 we numerically investigate the analyticity domains of periodic orbits and invariant curves using Padé approximants. A new method to determine the analyticity radius of the parametrizing function is presented in §4. A comparison with Greene's method and the root criterion is provided in §5. In §6 we briefly recall the predictions of renormalization theory, while in §7 we present several numerical results and the conclusions.

2 Perturbative series expansions for periodic orbits

We consider the standard map defined by the equations

$$\begin{aligned} r_{n+1} &= r_n + \varepsilon \sin\theta_n \\ \theta_{n+1} &= \theta_n + r_{n+1} \ , \end{aligned} \tag{1}$$

where $r_n \in \mathbf{R}$, $\theta_n \in \mathbf{R}/2\pi\mathbf{Z}$. By $\theta_{n+1} - \theta_n = r_{n+1}$ and $\theta_n - \theta_{n-1} = r_n$, one obtains

$$\theta_{n+1} - 2\theta_n + \theta_{n-1} = \varepsilon \sin\theta_n \ . \tag{2}$$

We look for a periodic solution with frequency $\omega = \frac{p}{q}$ (where $p, q \in \mathbf{Z}_+$), such that it satisfies the periodicity conditions

$$\begin{aligned} \theta_{n+q} &= \theta_n + 2\pi p \\ r_{n+q} &= r_n \ . \end{aligned} \tag{3}$$

We parametrize the solution as

$$\theta_n = \varphi_n + u(\varphi_n) \ , \qquad\qquad \varphi_n \in \mathbf{R}/2\pi\mathbf{Z} \ ,$$

where $u(\varphi_n)$ is $2\pi p$–periodic and where the flow is linear with frequency $\frac{p}{q}$: $\varphi_{n+1} = \varphi_n + 2\pi\frac{p}{q}$. With this choice of the parametrization, the periodicity conditions (3) are trivially satisfied. Let us expand the function u in Fourier–Taylor series as

$$u(\varphi_n) \ \equiv \ \sum_{j=1}^{\infty} \varepsilon^j \sum_{l=1}^{q} a_{lj} \sin(l\varphi_n) \ , \tag{4}$$

where the real coefficients a_{lj} will be determined by means of (2). The reason for which the sum over l runs from 1 to q will be clear from the choice of the *initial condition* φ_0, which must be selected so to avoid zero divisors. ¿From (2) it follows that the function u must satisfy the relation

$$u(\varphi_n + 2\pi\frac{p}{q}) - 2u(\varphi_n) + u(\varphi_n - 2\pi\frac{p}{q}) = \varepsilon \sin(\varphi_n + u(\varphi_n)) \ . \tag{5}$$

The coefficients a_{lj} are obtained inserting the series expansion (4) in (5) and equating same orders of ε. More precisely, one has

$$\begin{gathered} u(\varphi_n + 2\pi\frac{p}{q}) - 2u(\varphi_n) + u(\varphi_n - 2\pi\frac{p}{q}) \equiv \\ \equiv \sum_{j=1}^{\infty} \varepsilon^j \sum_{l=1}^{q} a_{lj} \ 2\sin(l\varphi_n) \ [\cos(2\pi l\frac{p}{q}) - 1] = \varepsilon \ \sin(\varphi_n + u(\varphi_n)) \ . \end{gathered} \tag{6}$$

To solve (6) recursively, let

$$u(\varphi_n) = \sum_{j=1}^{\infty} \varepsilon^j u_j(\varphi_n) \qquad \text{with} \qquad u_j(\varphi_n) = \sum_{l=1}^{q} a_{lj} \ \sin(l\varphi_n) \ . \tag{7}$$

Moreover, let

$$e^{i(\varphi_n + u(\varphi_n))} \equiv \sum_{m=0}^{\infty} b_m(\varphi_n)\varepsilon^m \ , \tag{8}$$

where the coefficients $b_m(\varphi_n)$ can be recursively computed as follows. Differentiating (8) w.r.t. ε and using the series expansion (7), one obtains

$$i \ \sum_{j=1}^{\infty} j\varepsilon^{j-1} u_j(\varphi_n) \cdot \sum_{m=0}^{\infty} b_m(\varphi_n)\varepsilon^m \ = \ \sum_{m=1}^{\infty} m b_m(\varphi_n)\varepsilon^{m-1} \ ,$$

from which it follows that the coefficients b_m are iteratively defined as

$$
\begin{aligned}
b_0(\varphi_n) &= e^{i\varphi_n} \\
b_m(\varphi_n) &= \frac{i}{m} \sum_{j=1}^{m} j u_j b_{m-j} \ , \qquad \forall m \geq 1 \ .
\end{aligned}
$$

Therefore, we can rewrite $\varepsilon \sin(\varphi_n + u(\varphi_n))$ as

$$
\varepsilon \sin(\varphi_n + u(\varphi_n)) \ = \ \frac{1}{2i} \sum_{m=1}^{\infty} \Big(b_{m-1}(\varphi_n) - \overline{b_{m-1}(\varphi_n)} \Big) \ \varepsilon^m \ .
$$

We can now proceed with the computation of the coefficients a_{lj} (such that $a_{-lj} = -a_{lj}$) from

$$
\begin{aligned}
u(\varphi_n + 2\pi \frac{p}{q}) - 2u(\varphi_n) + u(\varphi_n - 2\pi \frac{p}{q}) &= \\
&= \sum_{j=1}^{\infty} \varepsilon^j \frac{1}{2i} \sum_{l=-q, l\neq 0}^{q} 2a_{lj} e^{il\varphi_n} (\cos(2\pi l \frac{p}{q}) - 1) \\
&= \frac{1}{2i} \sum_{j=1}^{\infty} \varepsilon^j (b_{j-1}(\varphi_n) - \overline{b_{j-1}(\varphi_n)}) \ .
\end{aligned}
$$

Equating same orders of ε, one gets

$$
\sum_{l=1}^{q} 2a_{lj} (e^{il\varphi_n} - e^{-il\varphi_n}) \ (\cos(2\pi l \frac{p}{q}) - 1) = b_{j-1}(\varphi_n) - \overline{b_{j-1}(\varphi_n)} \ ,
$$

which defines the coefficients a_{lj} from the knowledge of the b_j's.

We remark that to the order ε^q, one has to select φ_n such that $\sin(q\varphi_n) = 0$; such choice compensates the zero term occurring in $\cos(2\pi q \ \frac{p}{q}) - 1$. This choice of φ_n fixes the value of φ_0, since $\varphi_n = \varphi_0 + 2\pi n \frac{p}{q}$. Correspondingly, one has the two solutions (modulus 2π):

$$
\varphi_0 = \frac{\pi}{q} \qquad \text{and} \qquad \varphi_0 = \frac{2\pi}{q} \ .
$$

One finds that the orbit starting at $\varphi_0 = \frac{\pi}{q}$ is stable for q odd and unstable for q even, while that starting at $\varphi_0 = \frac{2\pi}{q}$ is stable for q even and unstable for q odd. Let us stress that the coefficient a_{qq} appearing in the function $u_q(\varphi_n) = \sum_{l=1}^{q} a_{lq} \sin(l\varphi_n)$ is not determined by the above recursive formulae; however, this term does not contribute to the general solution, due to the choice of φ_0 such that $\sin(q\varphi_0) = 0$. In order to provide explicit formulae for the coefficients a_{lj} it is convenient to distinguish the cases $j < q$, $j = q$ and $j > q$. Below is the list of formulae where we have introduced some coefficients β_{lj} defined by the relation

$$\frac{1}{2i}(b_{j-1}(\varphi_n) - \overline{b_{j-1}(\varphi_n)}) \ \equiv \ \sum_{l=1}^{j} \beta_{lj} \sin(l\varphi_n) \ .$$

i) $j < q$: $a_{lj} = \frac{\beta_{lj}}{2[\cos(2\pi l \frac{p}{q})-1]}$ for $l = 1, ..., j$.

ii) $j = q$: $a_{lq} = \frac{\beta_{lq}}{2[\cos(2\pi l \frac{p}{q})-1]}$ for $l = 1, ..., q-1$.

iii) $j > q$: Let us introduce the coefficients $\tilde{\beta}_{lj}$ defined through the expression

$$\begin{aligned}\sum_{l=1}^{j} \beta_{lj} \sin(l\varphi_n) &= \sum_{l=1}^{q} \beta_{lj} \sin(l\varphi_n) + \sum_{l=q+1}^{j} \beta_{lj} \sin((l - [\frac{l}{q}]q)\varphi_n) \ \cos([\frac{l}{q}]q\varphi_n) \equiv \\ &\equiv \sum_{l=1}^{q} \tilde{\beta}_{lj} \sin(l\varphi_n) \ ,\end{aligned}$$

with $\beta_{nq,j} = 0$ for every $n \in \mathbf{Z}_+$. Then: $a_{lj} = \frac{\tilde{\beta}_{lj}}{2[\cos(2\pi l \frac{p}{q})-1]}$ for $l = 1, ..., q-1$.

The expressions *i)-iii)* determine uniquely the coefficients a_{lj} appearing in (4).

Remark 1 *The above formulae can be easily generalized to any standard–like map with* $\sin\theta_n$ *in (4) replaced by* $f(\theta_n) = \sum_{k=1}^{N} \alpha_k \sin(k\theta_n)$ *for any* $N \in \mathbf{Z}_+$ *and* $\alpha_k \in \mathbf{R}$. *One needs just to substitute* β_{lj} *with* $\sum_{k=1}^{N} \alpha_k \beta_{lj}^{(k)}$ *and to define* $\sum_{l=1}^{j} \beta_{lj}^{(k)} \sin(l\varphi_n) \equiv \frac{1}{2i}(b_{j-1}^{(k)}(\varphi_n) - \overline{b_{j-1}^{(k)}(\varphi_n)})$ *with*

$$\begin{aligned} b_0^{(k)}(\varphi_n) &\equiv e^{ik\varphi_n} \\ b_m^{(k)}(\varphi_n) &\equiv \frac{ik}{m} \sum_{j=1}^{m} j u_j b_{m-j}^{(k)} \ , \qquad \forall m \geq 1 \ .\end{aligned}$$

3 Singularities by Padé approximants

We consider the series

$$u(\varphi_0; \varepsilon) \ = \ \sum_{j=1}^{\infty} u_j(\varphi_0)\varepsilon^j \ , \tag{9}$$

Table 1

γ	ω_1	ω_2
1/2	1/3	10/21
2/3	12/37	11/23
3/5	13/40	21/44
5/8	25/77	32/67
8/13	38/117	53/111
13/21	63/194	85/178
21/34	101/311	138/289
34/55	164/505	223/467
55/89	265/816	361/756
89/144	429/1321	584/1223

where the coefficients $u_j(\varphi_0)$ have been defined in sect. 2. Let ε be a complex parameter; we compute Padé approximants (see, e.g., [4,5]) of order [200/200], where for consistency the coefficients $u_j(\varphi_0)$ have been calculated with a precision of 400 decimal digits. False poles have been discarded by comparison with the zero's generated by the Padé approximants. The analysis based on Pade's method allows to know the location of the singularities and, whether it exists, the shape of the analyticity domain. The radius of convergence of the parametrizing series is provided by the innermost singularity approaching the origin. We limit to the study of the periodic orbits associated to the continued fraction truncation of the noble numbers $\gamma = [1^\infty]$, $\omega_1 = [3, 12, 1^\infty]$, $\omega_2 = [2, 10, 1^\infty]$, where we denote by $[a_1, a_2, a_3, ...] = \frac{1}{a_1 + \frac{1}{a_2 + \frac{1}{a_3 + ...}}}$ and 1^∞ stands for an infinite tail of 1's. A list of the rational numbers we have considered, approximating γ, ω_1, ω_2, is given in Table 1.

We compute also Padé approximants for invariant curves, noticing that in analogy with periodic orbits, when ω is irrational one can introduce a parametrization of the invariant curve with rotation number ω as

$$\theta_n = \varphi_n + U(\varphi_n; \varepsilon), \qquad \varphi_n \in \mathbf{R}/2\pi\mathbf{Z} ,$$

with the property that $\varphi_{n+1} = \varphi_n + \omega$. The function U is obtained solving the equation

$$U(\varphi_n + \omega; \varepsilon) - 2U(\varphi_n; \varepsilon) + U(\varphi_n - \omega; \varepsilon) = \varepsilon \sin(\varphi_n + U(\varphi_n; \varepsilon)) \; ; \qquad (10)$$

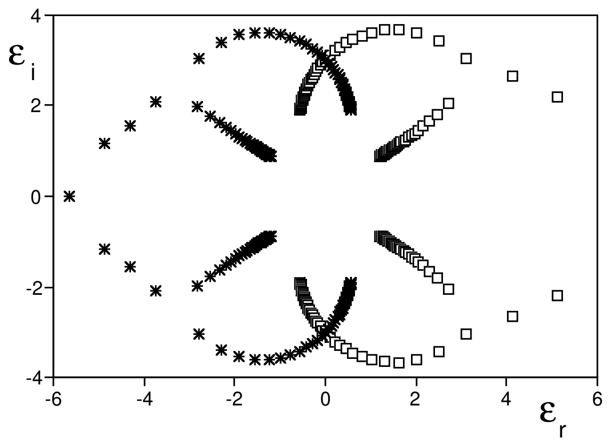

Fig. 1. Padé approximants of order [200/200] of the periodic orbit with frequency 3/5. Stars denote the stable periodic orbit (with $\varphi_0 = \frac{\pi}{5}$), while squares correspond to the unstable orbit (with $\varphi_0 = \frac{2\pi}{5}$).

in particular, the coefficients of the Lindstedt series

$$U(\varphi_n;\varepsilon) \;=\; \sum_{j=1}^{\infty} U_j(\varphi_n)\varepsilon^j \tag{11}$$

can be obtained by inserting the series expansion (11) in (10) and equating same orders of ε. Notice that in this case the function $U = U(\varphi_n;\varepsilon)$ depends explicitely on the parametric coordinate φ_n. A complete study of the domains of analyticity of γ, ω_1, ω_2 has been performed in [6].

In this section we are mainly concerned with singularities of the approximating periodic orbits. Figure 1 shows the Padé approximants [200/200] of the periodic orbit with $\frac{p}{q} = \frac{3}{5}$; stable periodic orbit (obtained by taking $\varphi_0 = \frac{\pi}{5}$) and the unstable orbit (with $\varphi_0 = \frac{2\pi}{5}$) are shown. Apparently the two graphs seems to be obtained by a reflection about the vertical axis; however, only very particular cases (e.g., $\frac{p}{q} = \frac{2}{3}$) are exactly symmetric. We note also that the shape of the line of singularities is very similar to that of a square root branch point, which suggests that the Padé approximants have a similar behaviour in the two cases: a deeper understanding of the nature of these singularities is presented in [13].

For the golden ratio γ, the analyticity domain as computed in [4,9] is shown to be approximately a circle with radius equal to 0.971635. Figure 2 shows the overlap of the Padé approximants of the stable and unstable periodic orbits $\frac{3}{5}$, $\frac{13}{21}$, $\frac{34}{55}$, $\frac{89}{144}$; the inner black domain corresponds to the irrational frequency γ. Other periodic orbits are not drawn to avoid overpopulation in the picture. We remark that the domains of the periodic orbits approach more and more

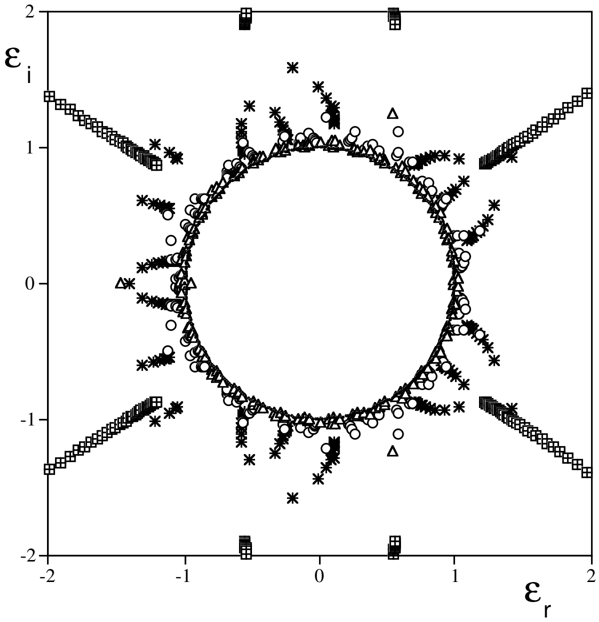

Fig. 2. Padé approximants of order [200/200] for some rational approximants to γ listed in Table 1. The inner circle denotes Padé approximants to the invariant curve with frequency γ. Stable and unstable periodic orbits 3/5 are denoted by a cross inside a square, 13/21 by a star, 34/55 by a circle, 89/144 by a triangle.

that of the irrational number as the order q of the periodic orbit grows.

We report in Figure 3 the Padé approximants corresponding to ω_1 and ω_2 and those of some rational approximants listed in Table 1. The innermost domain of black squares refers to the invariant curve.

Let us define the radius of convergence of the Lindstedt series (9) as

$$\rho_c(\frac{p}{q}) \ = \ \Big(\limsup_{j\to\infty} \ |u_j(\varphi_0)|^{1/j}\Big)^{-1} \ . \tag{12}$$

In a similar way, for ω irrational, we define the radius of convergence of the Lindstedt series (11) as

$$\rho_c(\omega) \ = \ \inf_{\varphi\in\mathbf{R}/2\pi\mathbf{Z}} \Big(\limsup_{j\to\infty} \ |U_j(\varphi)|^{1/j}\Big)^{-1} \ .$$

As a byproduct of our results for γ, ω_1, ω_2, we conjecture that

$$\lim_{k\to\infty} \rho_c(\frac{p_k}{q_k}) \ = \ \rho_c(\omega) \ ,$$

where $\{\frac{p_k}{q_k}\}$ are the rational approximants to ω. Figure 4 shows the radii of convergence of some rational approximants to the golden ratio γ. The dot-

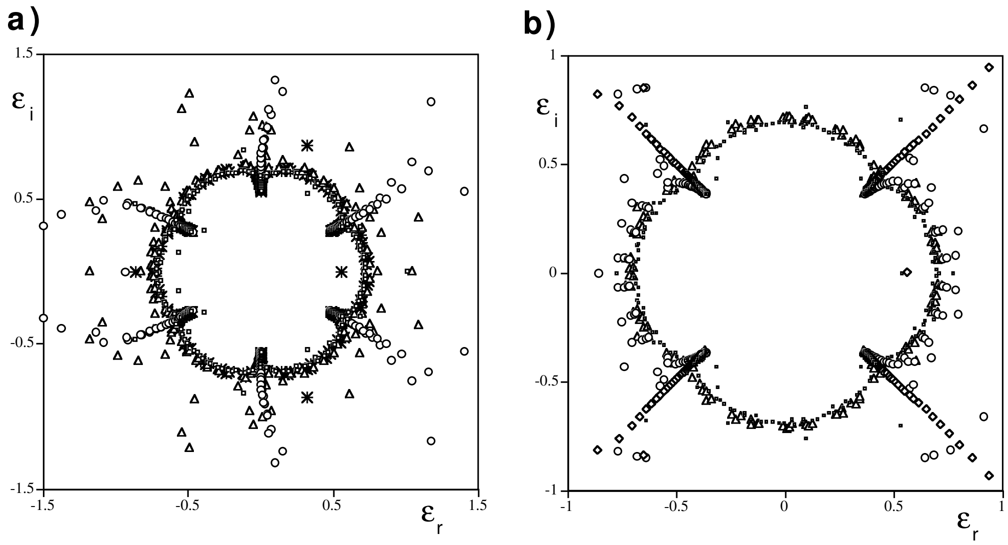

Fig. 3. Padé approximants of order [200/200] for the rational approximants to ω_1 and ω_2. The inner domain of small squares denotes Padé approximants to the invariant curve with frequency ω_1 in a) and ω_2 in b). a) : Stable and unstable 13/40 periodic orbits are represented by a circle, 25/77 by a triangle and 38/117 by a star. b) : 10/21 periodic orbits are represented by a diamond, 21/44 by a circle and 53/111 by a triangle.

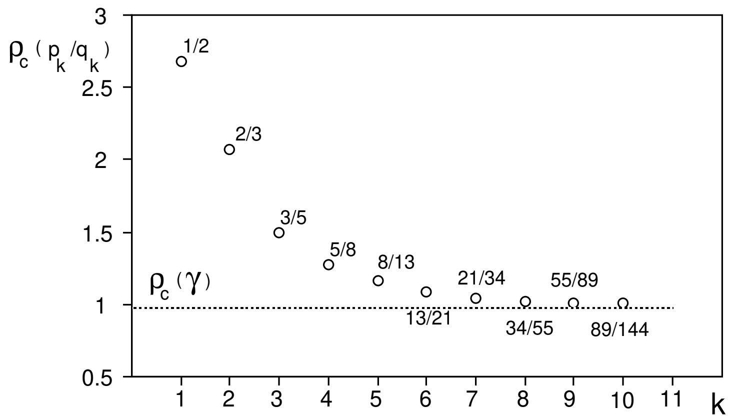

Fig. 4. The radius of convergence (12) vs. the order k of the rational approximants p_k/q_k to the golden ratio. The dotted line corresponds to the radius of convergence of the invariant curve with frequency γ.

ted line corresponds to the radius of convergence of γ as derived from Padé analysis.

Remark: The fact that the domains of the approximating periodic orbits tend to a limiting domain suggests that the location of the poles for the invariant curve does not depend on the specific value of the coordinate φ, which must have a definite (arbitrary) value in order to compute the Padé approximants.

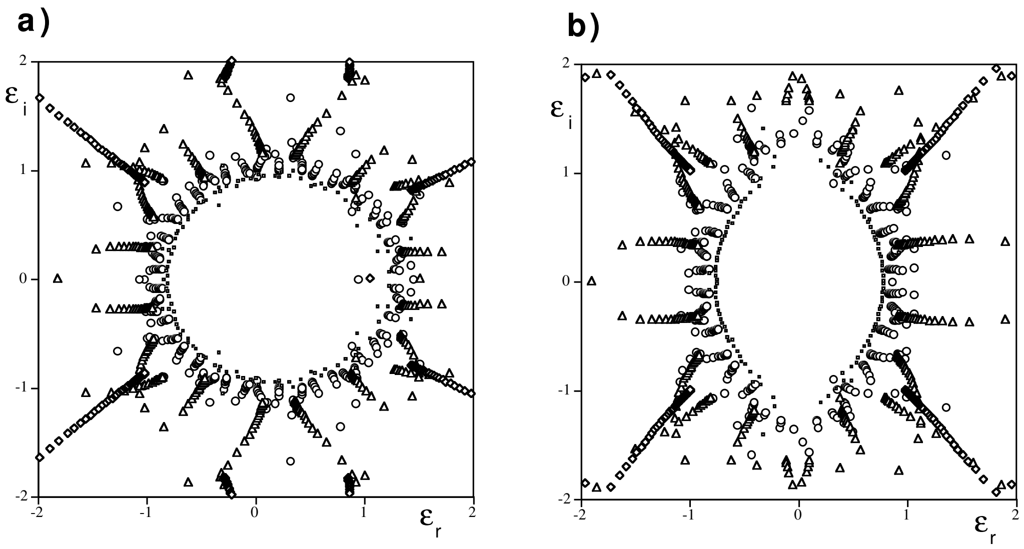

Fig. 5. Padé approximants of order [200/200] for the cases $a)$: f_{12} and $b)$: f_{13} and for some rational approximants to γ. The inner domain of small squares denotes Padé approximants to the invariant curve with rotation number γ. Periodic stable and unstable 3/5 orbits are represented by a diamond, 8/13 by a triangle, 21/34 by a circle.

It is possible to generalize the construction of the series expansion and the study of the domain of analyticity and singularities to the case of standard-like maps where the term $\sin\theta_n$ in (1) is replaced by a linear combination of $\sin k\theta_n$ for integer values of k. Formulae for the computation of the coefficients of the ε–expansion of the parametric solution for periodic orbits have been reported in §2. The construction depends only on parity properties of the map (1), which are preserved in this generalization. We will consider only two cases, say f_{12} and f_{13} already studied in previous papers ([5,9]):

$$
\begin{aligned}
f_{12}: \qquad & r_{n+1} = r_n + \varepsilon(\sin\theta_n + \frac{1}{20}\sin 2\theta_n) \\
& \theta_{n+1} = \theta_n + r_{n+1} \ , \\
f_{13}: \qquad & r_{n+1} = r_n + \varepsilon(\sin\theta_n + \frac{1}{30}\sin 3\theta_n) \\
& \theta_{n+1} = \theta_n + r_{n+1} \ .
\end{aligned}
$$

Analogously to Figure 2 for the standard map case and for the golden ratio γ, we show in Figure 5 for f_{12} and f_{13} how the singularities of periodic orbits approaching the invariant curve with rotation number γ come closer and closer to the boundary of the domain of analyticity of the invariant curve.

4 A method for determining the analyticity radius

In order to calculate an estimate of the radius of convergence of the series (9) (computed via a recursive algorithm up to a finite order N), one has to determine a threshold at which the series "starts to diverge": this is of course a difficult task if one wants to keep a sort of uniformity for different series in such a way that the procedure can be authomatized in a computer program. We propose the following algorithm: let us consider different values of the small parameter ε from an initial ε_{in} to a final ε_{fin} with a relative increment $(1+h)*\varepsilon$. We then calculate for any of these ε–values the distance d_j between the truncated series at order j calculated at ε with that at $(1+h)*\varepsilon$. More precisely, if $u^{(j)}(\varphi_0;\varepsilon) \equiv \sum_{k=1}^{j} u_k(\varphi_0)\varepsilon^k$, then

$$d_j = d_j(\varepsilon) \equiv |u^{(j)}(\varphi_0;(1+h)*\varepsilon) - u^{(j)}(\varphi_0;\varepsilon)| \ .$$

Finally, we calculate the sum

$$s_1 = s_1(\varepsilon) \equiv \frac{1}{N-1}\sum_{j=2}^{N} log\frac{d_j}{d_1} \ .$$

Alternatively one can consider the quantity

$$\tilde{s}_l = \tilde{s}_l(\varepsilon) \equiv \frac{1}{N-1}\sum_{j=2}^{N} log\frac{d_j}{d_{j-l}}$$

for different integer values of the lag parameter l. Then we plot the resulting picture of s_1 versus ε (as in Figure 6a). We call this method *Lyapunov's* for obvious reasons. All graphs of s_1 versus ε show an initial almost constant value of s_1 as ε is increased, followed by a small well and a sharp increase with almost linear behaviour.

Remark 2 The quantity s_1 (or equivalently $\tilde{s}_l$) depends on the choice of the initial datum φ_0 (namely, whether the orbit is stable or unstable). However, experiments have shown that the radius of convergence is approximately the same (up to the precision we are considering in this work) for the two orbits and therefore it does not really matter what orbit one selects for the computation of the indicator s_1 (or $\tilde{s}_l$).

Figure 6b shows a zoom on the well of Figure 6a. In order to select the ε–value representing the analyticity radius, we proceed as follows. Having fixed the maximal order N, at which the series is explicitely computed, and the increment h, we interpolate the points before the well with a straigth line. The critical value, say ε_L, is determined as the intersection of such line with

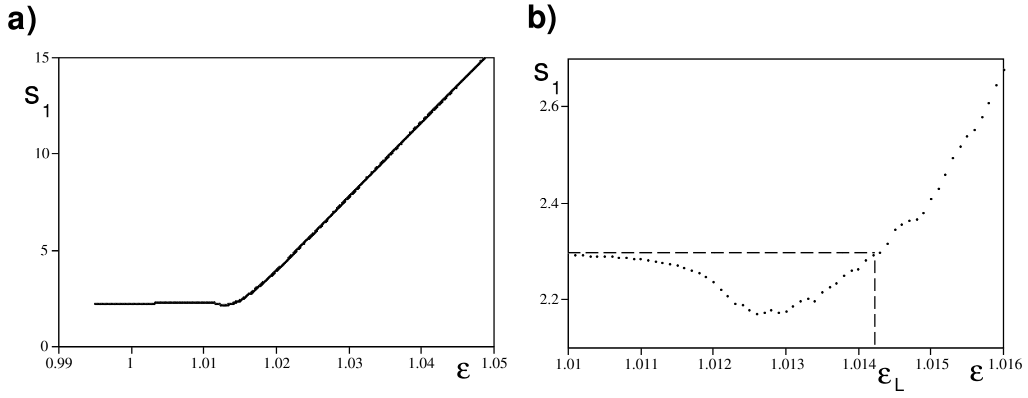

Fig. 6. a) Graph of s_1 versus ε for $p_k/q_k = 34/55$, $N = 800$, $h = 0.001$. b) Zoom of a) in the region $1.01 \leq \varepsilon \leq 1.016$. The selected value for the radius of convergence is denoted by ε_L.

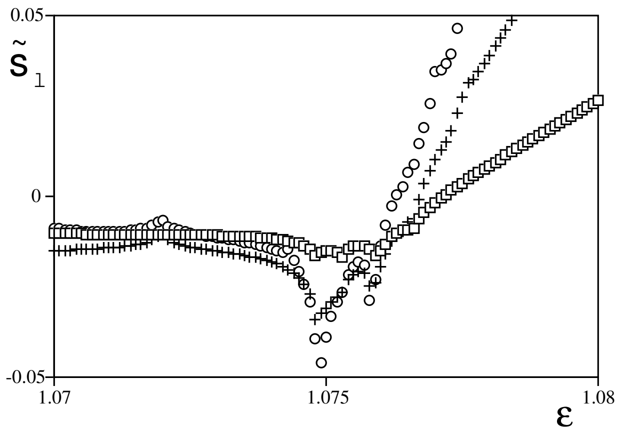

Fig. 7. Graph of $\tilde{s}_l$ vs. ε for $l = 10$ (squares), 30 (crosses), 50 (circles): 13/21 stable periodic orbit with $N = 800$ and $h = 0.001$.

the portion of the curve after the minimum is reached. This computation can be performed by an authomatic computer program that we develop to determine the critical ε_L for several different choices of n and h.

Instead of s_1 one can use the functions $\tilde{s}_l$ defined before. However, as shown in Figure 7 for $l = 10$, 30, 50, the curves are less regular compared with that obtained from s_1, eventhough the values of the proposed radius of analyticity are all very close together.

Remark 3 As an alternative method, we make some plots (as in [3]), where the effect of the truncation at order N in ε is controlled by means of a quantity which measures the distance between the actual and the approximate dynamics. More precisely, one can introduce the following quantities:

i) Iterate l times the standard map with initial data $(x_0 = \varphi_0 + u^{(N)}(\varphi_0), y_0 = \omega + u^{(N)}(\varphi_0) - u^{(N)}(\varphi_0 - \omega))$, where $u^{(N)}$ is the truncation at order N. Let (x_l, y_l) be the final point;

$ii)$ define (x_l, y_l) as $x_l = \varphi_0 + l\omega + u^{(N)}(\varphi_0 + l\omega)$, $y_l = \omega + u^{(N)}(\varphi_0 + l\omega) - u^{(N)}(\varphi_0 + l\omega - \omega)$.

Finally, let $d(N; \varepsilon)$ be the average distance over $l = 1, ..., L$ (for some integer L). This quantity provides an indication of the radius of convergence. As an example, we quote the 3/5 stable orbit: for $L = 800$ one finds that the quantity $d(N; \varepsilon)$ undergoes a sudden jump at approximately $\varepsilon = 1.33$ for $N = 100$ and $\varepsilon = 1.35$ for $N = 800$, which provides a result quite close to the other methods (compare with Greene's value of Table 2).

5 A comparison with Greene's method

Let $C_{\varepsilon,\omega}$ denote the invariant curve with irrational frequency ω for the standard mapping (1). Such curve exists for low values of ε and it becomes more and more distorted as ε grows, until one reaches a critical value at which $C_{\varepsilon,\omega}$ breaks down. Let us define the critical threshold as

$$\varepsilon_c(\omega) = \sup\{\varepsilon' \in \mathbf{R}_+ : \forall \varepsilon'' < \varepsilon' \ \exists \text{ an analytic invariant curve } C_{\varepsilon'',\omega}\} \ .$$

The most widely accepted numerical technique to compute $\varepsilon_c(\omega)$ is due to J. Greene ([10]). Greene's method is based on the idea that the break–down of an invariant curve $C_{\varepsilon,\omega}$ is strictly related to the transition from stability to instability of the periodic orbits with frequency equal to the rational approximants of ω.

To compute $\varepsilon_c(\omega)$ we need to study the stability of the approximating periodic orbits. To this end, for a fixed frequency $\frac{p}{q}$, we look at the eigenvalues of the matrix

$$M \ = \ \prod_{i=1}^{q} \begin{pmatrix} 1 + \varepsilon\cos(\theta_i) & 1 \\ \varepsilon\cos(\theta_i) & 1 \end{pmatrix} \ ,$$

where $(\theta_1, ..., \theta_n)$ are points on the periodic orbit. From the area–preserving property, $\det M = 1$. Let us denote by T the trace of M, $T \equiv Tr(M)$. If $|T| < 2$, the eigenvalues of M are complex conjugates on the unit circle and the periodic orbit is stable. On the contrary, if $|T| > 2$ the eigenvalues are real and the periodic orbit is unstable.

Let us consider the periodic orbit with frequency $\frac{p}{q}$, which is elliptic for small values of ε (as well as for $\varepsilon = 0$). As ε increases, the trace of the matrix M exceeds eventually 2 in modulus and the periodic orbit becomes unstable. We denote by $\rho_{Gr}(\frac{p}{q})$ the value of ε at which the transition from stability

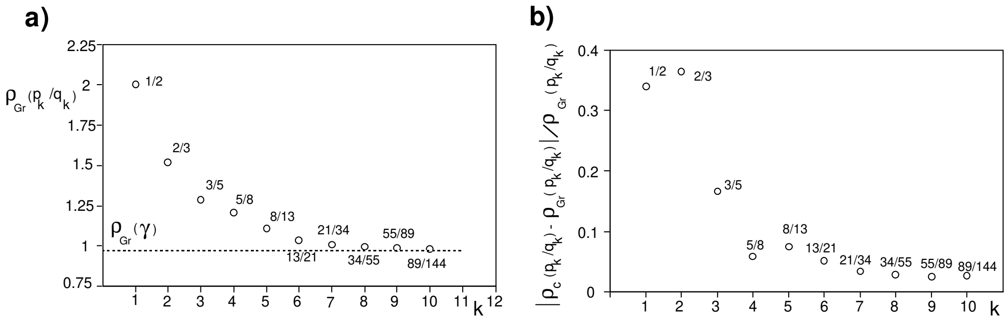

Fig. 8. *a*) : $\rho_{Gr}(\frac{p_k}{q_k})$ vs. the order k of the rational approximants p_k/q_k to the golden ratio. The dotted line corresponds to Greene's threshold for the golden mean invariant curve (i.e., $\rho_{Gr}(\gamma) = 0.971635$). *b*) : Relative error between $\rho_c(\frac{p_k}{q_k})$ and $\rho_{Gr}(\frac{p_k}{q_k})$ for some rational approximants to the golden ratio.

to instability occurs. We report in Figure 8a the value of $\rho_{Gr}(\frac{p_k}{q_k})$ for some approximants $\frac{p_k}{q_k}$ to the golden ratio; the dotted line denotes the break–down value of $C_{\varepsilon,\omega}$.

A proof of Greene's criterion would imply that the radius of convergence $\rho_c(\frac{p}{q})$ coincides with the loss of stability $\rho_{Gr}(\frac{p}{q})$. This property does not hold in general for low order periodic orbits, though the relative difference of the two values becomes smaller as the order of the approximant increases (compare with Figure 8b). However, we conjecture that the two values $\rho_c(\frac{p}{q})$ and $\rho_{Gr}(\frac{p}{q})$ tend to the same limit as $j \to \infty$. From the analysis of the domains of analyticity using Padé approximants, we infer that Greene's value can be identified with the intersection of the domain of analyticity of $C_{\varepsilon,\omega}$ with the positive real axis.

6 Link with renormalization theory

It is rather instructive to link the results obtained with the method introduced in the previous sections with renormalization theory. Let γ be the golden ratio and denote by $\{\frac{p_k}{q_k}\}$ the sequence of rational approximants to γ. With reference to §5, let $\rho_{Gr}^{(k)} = \rho_{Gr}(\frac{p_k}{q_k})$ be the value of the perturbing parameter at which the character of the periodic orbit with frequency $\frac{p_k}{q_k}$ changes from elliptic to hyperbolic. Renormalization theory predicts that the sequence $\{\rho_{Gr}^{(k)}\}$ converges asymptotically to the critical break–down value (at which the invariant curve with rotation number γ disappears) at a rate $1/\delta$ with $\delta = 1.62795$ (see [1], [14]). In other words, one finds ([1]) that the quantity

$$\frac{\rho_{Gr}^{(k-1)} - \rho_{Gr}^{(k)}}{\rho_{Gr}^{(k)} - \rho_{Gr}^{(k+1)}} \to \delta \qquad \text{as} \quad k \to \infty \ .$$

In terms of renormalization group analysis, δ corresponds to the positive largest eigenvalue of the unstable manifold at the critical (non trivial) fixed point.

By replacing $\rho_{Gr}^{(k)}$ with the critical value $\rho_{Lyap}^{(k)}$ obtained implementing the Lyapunov method of §4, one expects that $\rho_{Lyap}^{(k)}$ rescales at rate $1/\delta$. A similar result should be valid taking the sequence $\{\rho_{Pade}^{(k)}\}$ obtained by Padé approximants. Notice that the critical value δ appears to be independent of the mapping, in the sense that one should find similar results for the standard mapping or for the maps f_{12}, f_{13}.

For the investigation of rotation numbers different from γ, it is useful to mention the existence of two more eigenvalues: $\delta_1 = -2.68174$ which is another eigenvalue at the non trivial fixed point and $\lambda = -2.61803$ which is an eigenvalue at the trivial fixed point (see [1,14]).

7 Results and conclusions

We investigate the analyticity property of the golden mean invariant curve and of the approximating periodic orbits for the standard map and the mappings f_{12}, f_{13}. Moreover we perform the same analysis for the standard map with irrational numbers $\omega_1 = [3, 12, 1^\infty]$, $\omega_2 = [2, 10, 1^\infty]$ and their rational approximants listed in Table 1. Three methods have been implemented, namely Padé approximants, Greene's criterion and the method introduced in §4 to which we refer as Lyapunov method. All these techniques depend on the choice of some parameters and/or tolerance errors. The choice of these quantities have been widely discussed in the literature in the cases of Greene and Padé. Lyapunov method depends on the order N of the truncation of the parametrizing series and the increment h of the perturbing parameter ε. We report in Table 2 the comparison of the three methods for the golden ratio approximants of the standard map. The series have been computed up to $N = 800$ and we let the increment vary taking $h = 10^{-1}, 10^{-2}, 10^{-3}, 10^{-4}$. The last row denotes a linear fit of the data to check the rate of convergence as predicted by renormalization group analysis. More precisely, if $\{\varepsilon_j\}$ denote the values in one of the columns corresponding to Greene, Padé or Lyapunov, we compute a linear fit of the data $\{\log(\varepsilon_j - \varepsilon_c)\}$, where ε_c denotes the critical break–down value of the limit invariant curve (i.e., $\varepsilon_c = 0.971635$). We recall that the theoretical prediction of renormalization theory ([1,14]) is $\varepsilon = \log(1/1.62795) \simeq -0.487321$.

In all cases considered in the present work, the Lyapunov values are not affected using an absolute increment of the same size (that is using $\varepsilon_2 = \varepsilon_1 + h$

Table 2

p/q	Greene	Padé	Lyap.:$h = 0.1$	$h = 10^{-2}$	$h = 10^{-3}$	$h = 10^{-4}$
$2/3$	1.5176	2.0501	1.8826	2.0445	2.0584	2.0590
$3/5$	1.2856	1.4873	1.3639	1.4812	1.4913	1.4920
$5/8$	1.1485	1.2495	1.1488	1.2478	1.2561	1.2568
$8/13$	1.0790	1.1440	1.0508	1.1413	1.1492	1.1497
$13/21$	1.0353	1.0753	0.9852	1.0698	1.0766	1.0772
$21/34$	1.0106	1.0366	0.9507	1.0327	1.0397	1.0403
$34/55$	0.9953	1.0115	0.9270	1.0073	1.0142	1.0147
$55/89$	0.9862	0.9974	0.9117	0.9899	0.9960	0.9966
$89/144$	0.9832	0.9909	0.9046	0.9831	0.9897	0.9901
Fit	-0.4944	-0.4991	-1.0014	-0.5543	-0.5054	-0.5025

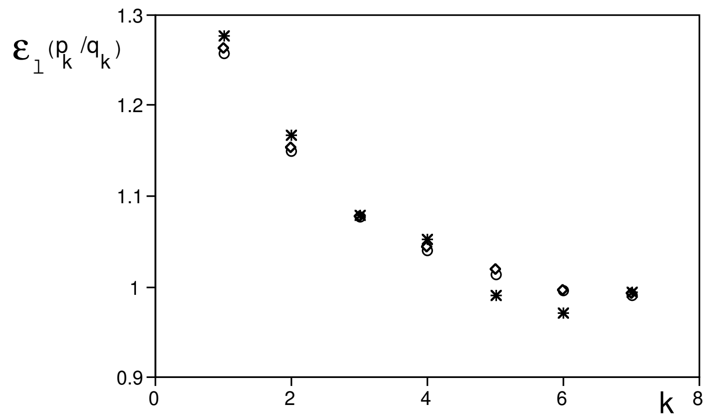

Fig. 9. Lyapunov values ε_l for the approximants 5/8, ..., 89/144 to the golden mean curve of the standard mapping for different values of the order of the expansion $N = 200$ (stars), 400 (diamonds), 800 (circles) and $h = 0.001$.

instead of $\varepsilon_2 = \varepsilon_1 * (1+h)$ in the algorithm). One can conclude that for a fixed N the agreement of the three methods is almost optimal taking $h = 0.001$, being almost the best considered. More precisely, the Lyapunov threshold decreases as N increases and it decreases as h increases. To see what is the effect of varying the order of truncation N, we report in Figure 9 the Lyapunov values $\varepsilon_l(\frac{p_k}{q_k})$ obtained for $N = 200$, 400, 800, again for the approximants $\frac{p_k}{q_k}$ to the golden mean curve of the standard map (here $h = 0.001$). The first two approximants (2/3 and 3/5) have been omitted from the figure to simplify the drawing.

The results in the case of the standard map for the noble numbers $\omega_1 = [3, 12, \gamma]$ and $\omega_2 = [2, 10, \gamma]$ are listed respectively in Table 3 and Table 4 with

Table 3

p/q	Greene	Padé	$Lyap(1.01)$	$Lyap(1.001)$
12/37	0.7486	0.5730	0.57154	0.57513
13/40	0.7322	0.5447	0.54309	0.54658
25/77	0.7232	0.5579	0.56070	0.56063
38/117	0.7145	0.5539	0.55230	0.55580
63/194	0.7134		0.55403	0.55755
101/311	0.7085		0.55315	0.55688
164/505	0.7073		0.55341	0.55715
265/816	0.7066		0.55358	0.55706
429/1321	0.7056		0.55345	0.55705
FIT	-0.5736			-2.6 – -2.7

the order of expansion $N = 800$. We report also the values of the fits for the different methods. The fit for Greene method is computed as in Table 2. We do not report any fit for Padé method due to the limited number of results available and for Lyapunov, case $h = 0.01$, since the data are not good as the increment is too large. Concerning the Lyapunov method, we stress that the corresponding values do not decrease monotonically, but rather oscillate around a critical value. Therefore we compute a fit of the data corresponding to the periodic orbit with frequency $\frac{p_k}{q_k}$ with a function of the form $1/(-a)^k$ for some positive real number a. The value reported in Table 3 and 4 is an approximate estimate of a. Notice that to obtain such estimate, the computations for Lyapunov values have been extended to one more decimal digit; moreover, the values corresponding to 12/37 in Table 3 and to 10/21 in Table 4 have been discarded, since they do not fit very well with the other data.

We present now the study of the two standard–like mappings f_{12} and f_{13} of §3. The results are summarized in Figure 10. The abscissa k refers to the approximant p_k/q_k, between 2/3 and 89/144, of the golden ratio, whose break–down threshold as computed by Greene's method amounts to $\varepsilon(f_{12}) = 1.2166$ and $\varepsilon(f_{13}) = 0.7545$. The Lyapunov method has been applied with a series truncated at $N = 800$. Results for two different values of the increment (i.e., $h = 0.01$ and $h = 0.001$) are presented. Padé approximants of order [200/200] have been computed. Due to the length of the calculation required by Padé method only the first few approximants (up to 21/34) have been analyzed.

Table 4

p/q	Greene	Padé	$Lyap(1.01)$	$Lyap(1.001)$
10/21	0.7487	0.5395	0.53805	0.54165
11/23	0.7198	0.5008	0.49223	0.49557
21/44	0.7060	0.5158	0.51449	0.51795
32/67	0.6919	0.5084	0.50703	0.51058
53/111	0.6869	0.5116	0.51007	0.51354
85/178	0.6842	0.5105	0.50893	0.51239
138/289	0.6801		0.50938	0.51281
223/467	0.6785		0.50921	0.51265
361/756	0.6781		0.50925	0.51271
584/1223	0.6771		0.50926	0.51268
FIT	-0.5254			-2.6 – -2.7

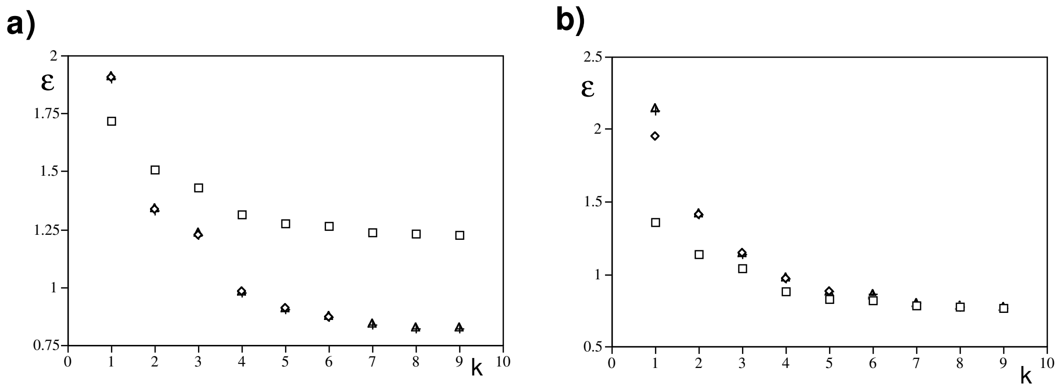

Fig. 10. Results for the mapping f_{12} (a), f_{13} (b) and for some rational approximants to the golden ratio. Greene's values are represented by a square, Padé by a diamond, Lyapunov for $h = 0.01$ by a cross and Lyapunov for $h = 0.001$ by a triangle.

Fits of the data are still in good agreement with renormalization theory. The values for the two mappings are reported in Table 5. The fit over Greene's data is performed using the values of the stable orbits. Concerning f_{13} we assume that the limiting threshold, as derived from higher order computations by Greene's method, is about 0.7545. In the case of the mapping f_{12} one has two values: the largest one is about 1.2166, while the smallest (derived from Greene's application changing ε in $-\varepsilon$ in the definition of the mapping f_{12}) is about 0.8050.

The results presented in this section show that there is a good agreement between all methods as far as the approximants to the golden mean curve of

Table 5

	f_{12}	f_{13}
Greene	-0.5037	-0.4967
Padé	-0.5570	-0.5491
Lyap. ($h = 0.01$)	-0.5409	-0.5429
Lyap. ($h = 0.001$)	-0.5076	-0.5124

the standard map are investigated. In this case the domain of analyticity in the complex ε–plane is close to a circle: therefore the intersection with the positive real axis (whose value is provided by Greene's technique) almost coincides with the analyticity radius (as given by Padé and Lyapunov's methods). A different situation occurs when the analyticity domain deviates from a circle, as for the invariant curves with rotation numbers $\omega_1 = [3, 12, 1^\infty]$ and $\omega_2 = [2, 10, 1^\infty]$. In these cases two thresholds appear: the positive real break–down threshold and the analyticity radius. As far as the golden mean is considered, independently from the equations of the mapping, the values provided by all methods for the various approximants (as listed in Table 1) rescale by a factor about equal to -0.5, which coincides with the logarithm of the inverse of the largest eigenvalue of the unstable manifold at the critical fixed point as predicted by renormalization theory. A different situation appears as γ is replaced by ω_1 or ω_2 for which two different thresholds can be defined: Greene's value (coinciding with the intersection of the analyticity domain with the positive real axis) and the analyticity radius. Our analysis shows that one finds two different rates of convergence; Greene's method is still related to δ, while Lyapunov and Padé methods rescale at a rate between 2.6 and 2.7. We cannot determine with more accuracy this latter rescaling value, due to the fact that the fit is performed over too few data. However, we conjecture that the rescaling of Lyapunov could be related to the eigenvalue $\delta_1 = -2.68174$ at the non trivial fixed point or to the eigenvalue $\lambda = -2.61803$ at the trivial fixed point. We plan to investigate this phenomenon in more detail in a future work.

Acknowledgements

We are deeply indebted to J.–P. Eckmann for interesting suggestions and discussions during the accomplishment of this work. We would like to thank also G. Benfatto, A. Berretti, G. Gallavotti, G. Gentile, H. Koch, R. de la Llave, C. Simó and P. Wittwer for many helpful discussions and advices.

References

[1] J.J. Abad, H. Koch and P. Wittwer, A renormalization group for Hamiltonians: numerical results, *Nonlinearity* **11** (1998) 1185–1194.

[2] G. Baker and M. Graves-Morris, *Padé Approximants* (Addison-Wesley, 1981).

[3] G. Benettin, G. Turchetti and G. Zanetti, Critical behaviour of invariant curves in the standard map: a perturbative approach, *Physics Letters* **105A**, n. 9 (1984) 436–438.

[4] A. Berretti and L. Chierchia, On the complex analytic structure of the golden invariant curve for the standard map, *Nonlinearity* **3** (1990) 39–44.

[5] A. Berretti, A. Celletti, L. Chierchia and C. Falcolini, Natural boundaries for area preserving twist maps, *J. Stat. Phys.* **66** (1992) 1613–1630.

[6] A. Berretti, C. Falcolini and G. Gentile, Shape of analyticity domains of the Lindstedt series: The standard map, *Phys. Rev. E* **63** (2001).

[7] A. Berretti and S. Marmi, Standard map at complex rotation numbers: Creation of natural boundaries, *Phys. Rev. Lett.* **68** (1992) 1443–1446.

[8] C. Falcolini and R. de la Llave, A rigorous partial justification of Greene's criterion, *J. Stat. Phys.* **67** 609–643 (1992).

[9] C. Falcolini and R. de la Llave, Numerical calculation of domains of analyticity for perturbation theories in the presence of small divisors, *J. Stat. Phys.* **67** (1992) 645–666.

[10] J.M. Greene, A method for determining a stochastic transition, *J. Math. Phys.* **20** (1979).

[11] J. Roels and M. Hénon, Recherche des courbes invariantes d'une transformation ponctuelle plane conservant les aires, *Bull. Astron. Soc.* **2** (1967) 267–284.

[12] R. de la Llave and S. Tompaidis, Computation of domains of analyticity for some perturbative expansions of mechanics, *Physica D* **71** (1994) 55–81.

[13] R. de la Llave and S. Tompaidis, Nature of Singularities for Analyticity Domains of Invariant Curves, *Phys. Rev. Lett.* **73** (1994) 1459–1462.

[14] R.S. McKay, A renormalization approach to invariant circles in area preserving maps, *Physica* **7D** (1983) 283–300.

[15] R.S. McKay, On Greene's residue criterion, *Nonlinearity* **5** (1992) 161–187.

[16] H. Poincaré, *Les méthodes nouvelles de la méchanique céleste* (Gauthier Villars, Paris, 1899).

[17] J. Wilbrink, Erratic behaviour of invariant circles in standard-like mappings, *Phisica* **26D** (1987) 358–368.